

# Characterization of the Wallerian degeneration process in the rat spinal cord with DIAMOND and NODDI: comparison with histological observations.

Damien Jacobs<sup>1</sup>, Benoit Scherrer<sup>2</sup>, Aleksandar Jankovski<sup>3</sup>, Anne des Rieux<sup>4</sup>, Maxime Taquet<sup>1</sup>, Bernard Gallez<sup>4</sup>, Simon K. Warfield<sup>2</sup>, and Benoit Macq<sup>1</sup>  
<sup>1</sup>ICTEAM, Université catholique de Louvain, Louvain-La-Neuve, Belgium, <sup>2</sup>Computational Radiology Laboratory, Boston Childrens Hospital, Massachusetts, United States, <sup>3</sup>Hopital universitaire Mont-Godinne, Université catholique de Louvain, Godinne, Belgium, <sup>4</sup>LDRI, Université catholique de Louvain, Brussels, Belgium

**Purpose:** To investigate changes in DIAMOND<sup>1</sup> and NODDI<sup>2</sup> diffusion compartment imaging (DCI) models parameters after Wallerian degeneration of the spinal cord in rats and to compare findings with histology.

**Methods:** A left-unilateral rhizotomy was performed on 6 rats at L2-L3 levels, inducing Wallerian degeneration in the ipsilateral gracile fasciculus. A laminectomy was also performed on 3 control rats at identical L2-L3 levels. For each rat, diffusion weighted imaging (DWI) was performed at 11.7T, in vivo, after 51 days post-injured with 12 non-weighted DW images and 6 shells of 36 gradients directions each at b-values: 300, 700, 1500, 2800, 4500, 6000 s/mm<sup>2</sup>, non collinear directions<sup>3</sup>, voxel resolution: 0.1x0.1x1 mm<sup>3</sup>, TE: 23ms,  $\delta$ : 4.5ms,  $\Delta$ : 12 ms. After the acquisition, rats were perfused, spinal cord was removed, cryoprotected before being frozen and stored at -80°C, sliced axially in 20  $\mu$ m thick section using cryostat. Four immunostainings and one stain were performed for the myelin (LFB), neurofilaments (SMI312), oligodendrocytes (ab7474), microglia (Iba1), and astrocytes (GFAP). For each imaging dataset, DW images were resampled to 0.1x0.1x0.1mm<sup>3</sup> and corrected for animal motion and eddy-current distortion using affine registration to the b=0 s/mm<sup>2</sup> image. DIAMOND's and NODDI's model parameters were estimated using respectively the CRL Toolkit and the NODDI MATLAB library, considering one isotropic compartment and one anisotropic compartments for each model. NODDI models the diffusion arising from a fascicle using a Watson distribution of orientations of sticks with fixed axial diffusivity and null radial diffusivity, the concentration parameter of which provides a measure of the axonal orientation dispersion (orientation dispersion index, *odi*). In contrast, DIAMOND estimates all the parameters of a continuous peak-shaped 6-D distribution of diffusion tensors for each compartment. The concentration of the distribution provides a measure of the overall heterogeneity of the corresponding compartment (heterogeneity index, *hei*); the expectation of the distribution reflects the overall compartment diffusivity, providing, for each fascicle, diffusivity parameters ( $\lambda_{\parallel}$ ,  $\lambda_{\perp}$ ) that are not prefixed but estimated from the data. In this work, we also estimated the ADC for the isotropic compartment ( $D_{iso}$ ). DIAMOND and NODDI model parameters were compared in identical ROIs (~5000 voxels) drawn in the ipsilateral and contralateral parts of the spinal cords. For each diffusion model, we tested whether average parameter values in the ipsilateral and contralateral parts of the spinal cord were significantly different after rhizotomy and compared to sham rats. Due to the non-normality of the data's (normality test evaluation), the Kruskal-Wallis test was performed and combined with a multi comparison post-hoc test (Tukey-Kramer) to determine the statistical significance (with  $\alpha=0.05$ ) between the shams, contralateral and ipsilateral groups.

**Results: DIAMOND:** In the sham rats (Fig 1: i, red color), the estimated  $\lambda_{\parallel}$  of the fascicle was close to the known diffusivity of free diffusion value at 37°C (3  $\mu$ m<sup>2</sup>/ms). After rhizotomy, we observed a significant decrease in  $\lambda_{\parallel}$  and a significant increase in  $\lambda_{\perp}$  in the ipsilateral part (iii, green color). We also observed a significant increase in *hei* in the ipsilateral and contralateral parts (ii, blue color). The value of  $D_{iso}$  in the ipsilateral part decreased significantly and its fraction increased significantly ( $fD_{iso}$ ). **NODDI:** After rhizotomy, we observed a significant decrease of the intra-cellular volume fractions (*ficvf*) and the isotropic volume fraction (*fiso*) in the ipsilateral part. We also observed a significant increase in *odi*. **Histological analysis:** Axonal degeneration was observed in the ipsilateral part compared to the contralateral part (Fig 2.b vs 2.c, neurofilament staining). The fibrous structure of the myelin was observed in the contralateral part (Fig 2.d) but not preserved in the ipsilateral part (see structural dots, Fig 2.e). The process of myelin clearance was observed and confirmed with the microglia staining with a vesicular activation (Fig 2.f vs 2.g).

**Discussion:** DIAMOND and NODDI both detected an increased heterogeneity of the tissue microstructure after rhizotomy (significant increased *odi* and *hei*, Fig.1). However, with NODDI, the increased heterogeneity is described as an axonal orientation dispersion increase, which is difficult to interpret in the spinal cord. In contrast, DIAMOND provides an overall measure of heterogeneity of 3-D diffusivities in compartments and estimates diffusivity parameters for each compartment, providing further insight into the tissue microstructure *in vivo*. With DIAMOND, the increased  $\lambda_{\perp}$  is consistent with the altered fibrous structure and the myelin clearance process (Fig.2e). The decreased  $D_{iso}$  is consistent with the presence of both free diffusion and isotropic restricted diffusion due the vesicular activation (Fig.2g), captured together by the isotropic compartment. The increased  $fD_{iso}$  is consistent with the axonal degeneration (Fig.2c) during the Wallerian degeneration process.

**Conclusion:** Because in NODDI a number of parameters are fixed, variation of the DW signal due to a pathology are captured by the only remaining free model parameters, and the interpretation of these parameters is unclear. In contrast, DIAMOND estimates an overall measure of microstructural heterogeneity that can be further characterized by the estimated diffusivity parameters for each compartment. We found that  $D_{iso}$ ,  $fD_{iso}$  and  $\lambda_{\perp}$  reflect the Wallerian degeneration process.

[1]. Scherrer, B., et al., Characterizing the Distribution of Anisotropic Micro-structural environments with Diffusion-weighted imaging (DIAMOND). MICCAI, 2013. 16: p. 518-526. [2]. Zhang, H., et al., NODDI: practical in vivo neurite orientation dispersion and density imaging of the human brain. Neuroimage, 2012. 61(4): p. 1000-16. [3]. Caruyer, E., et al., Design of multishell sampling schemes with uniform coverage in diffusion MRI. Magn Reson Med, 2013. 69(6): p. 1534-40.

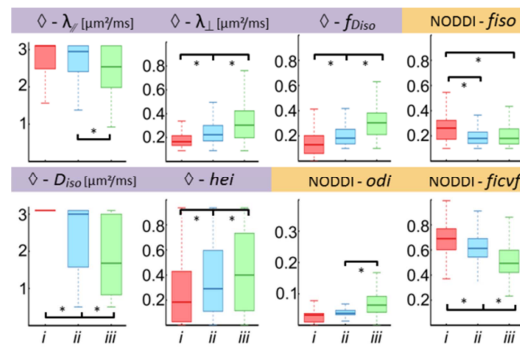


Figure 1 DIAMOND and NODDI parameters for the sham rats (i, red color), the contralateral part (ii, blue color) and the ipsilateral part (iii, green color). For DIAMOND:  $\lambda_{\parallel}$ ,  $\lambda_{\perp}$ : axial and radial diffusivities, *hei*: heterogeneity index,  $D_{iso}$ : Diffusion isotropic, and  $fD_{iso}$ : fraction of  $D_{iso}$ . For NODDI: *ficvf*: intra-cellular volume fraction, *fiso*: CSF volume fraction and *odi*: orientation dispersion index. \*: statistically significant

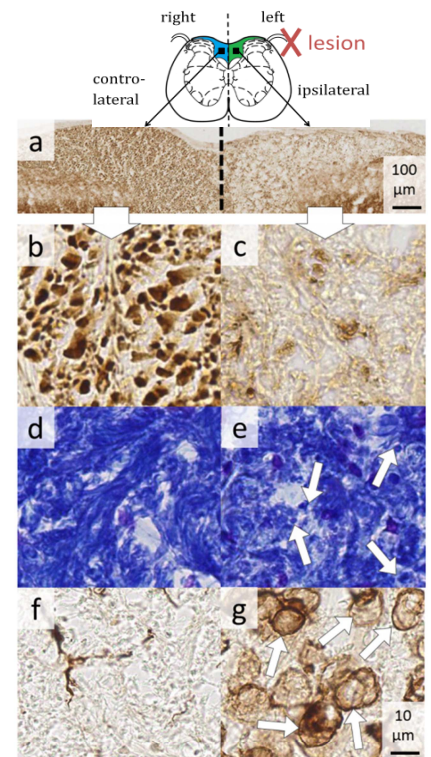


Figure 2 Immunostaining in the contralateral (left, blue color) and ipsilateral part (right, blue color) of the gracile fasciculus. (a-b-c) neurofilament (SMI-312), (d-e) LFB staining for the myelin, (f-g) Microglia staining (Iba-1) Scale bars: 100  $\mu$ m and 10  $\mu$ m.